

# 000 001 002 003 004 005 006 007 008 009 010 011 012 013 014 015 016 017 018 019 020 021 022 023 024 025 026 027 028 029 030 031 032 033 034 035 036 037 038 039 040 041 042 043 044 045 046 047 048 049 050 051 052 053 HERS: HIDDEN-PATTERN EXPERT LEARNING FOR RISK-SPECIFIC VEHICLE DAMAGE ADAPTATION IN DIFFUSION MODELS

Anonymous authors

Paper under double-blind review



Figure 1: Qualitative comparison of **HERS** against existing diffusion-based baselines. Observe that **HERS** generates damage regions with higher visual fidelity and localized consistency. Fine-grained artifacts such as dents, cracks, and abrasions are better preserved—zoom in for enhanced visibility of subtle and complex damage patterns.

## ABSTRACT

Recent advances in text-to-image (T2I) diffusion models have enabled increasingly realistic synthesis of vehicle damage, raising concerns about their reliability in automated insurance workflows. The ability to generate crash-like imagery challenges the boundary between authentic and synthetic data, introducing new risks of misuse in fraud or claim manipulation. To address these issues, we propose **HERS (Hidden-Pattern Expert Learning for Risk-Specific Damage Adaptation)**, a framework designed to improve **fidelity, controllability, and domain alignment** of diffusion-generated damage images. HERS fine-tunes a base diffusion model via **domain-specific expert adaptation**, without requiring manual annotation. Using self-supervised image–text pairs automatically generated by a large language model and T2I pipeline, HERS models each damage category—such as dents, scratches, broken lights, or cracked paint—as a separate expert. These experts are later integrated into a unified multi-damage model that balances specialization with generalization. We evaluate HERS across four diffusion backbones and observe **consistent improvements: +5.5% in text faithfulness and +2.3% in human preference ratings** compared to baselines. Beyond image fidelity, we discuss **implications for fraud detection, auditability, and safe deployment** of generative models in high-stakes domains. Our findings highlight both the opportunities and risks of domain-specific diffusion, underscoring the importance of trustworthy generation in safety-critical applications such as auto insurance.

054 **1 INTRODUCTION**

055

056 Text-to-image (T2I) diffusion models Saharia et al. (2022); Rombach et al. (2022); Podell et al. (2024);  
 057 Kang et al. (2023); Ramesh et al. (2021); Yu et al. (2023); Chang et al. (2023) have transformed  
 058 generative AI, producing photorealistic images from free-form language prompts and enabling rapid  
 059 advances in creative design, simulation, and data augmentation. Yet, when deployed in *safety-critical*  
 060 *domains* such as auto insurance, where every pixel may encode liability, their limitations become  
 061 clear. Generic T2I systems often fail to capture fine-grained damage categories—such as a dented  
 062 bumper, a subtle scrape across a door, or a fractured headlight—generating outputs that are visually  
 063 appealing but semantically unreliable (shown in Figure 1). In an insurance workflow, such errors are  
 064 not cosmetic: they can distort liability assessments, misinform fraud detection, and erode trust in  
 065 automated claims pipelines.

066 This duality makes generative models both an opportunity and a risk. On one hand, synthetic damage  
 067 data could dramatically improve training for rare-event modeling, accelerate claims assessment,  
 068 and expand coverage of long-tail accident cases. On the other hand, the same technology could be  
 069 exploited to fabricate fraudulent crash evidence or manipulate claims with high-fidelity synthetic  
 070 images. **To resolve this tension (raised in W1), we explicitly frame our goal: HERS is *not* intended to**  
 071 **generate “better fakes,” but rather to provide semantically faithful, liability-aware synthetic variations**  
 072 **that help insurance AI systems recognize both genuine and tampered evidence.** Unlike traditional  
 073 vision benchmarks, insurance scenarios require *risk-specific generation*, where semantic alignment,  
 074 forensic plausibility, and liability-aware consistency are as important as photorealism.

075 Prior approaches attempt to mitigate these issues via supervised fine-tuning Dai et al. (2023);  
 076 Segalis et al. (2023), human preference optimization Xu et al. (2023a); Fan et al. (2023), or spatial  
 077 grounding Li et al. (2023); Xie et al. (2023). However, these strategies are annotation-heavy and  
 078 often brittle, struggling to encode the hidden cues that forensic experts rely upon: the faint crease  
 079 from a low-speed collision, the asymmetric shattering of a headlight, or the implausible geometry of  
 080 tampered paint. **Furthermore, existing pipelines lack mechanisms for domain-structured adaptation**  
 081 **(W3), making them difficult to extend to multi-damage synthesis or to evaluate against risk-specific**  
 082 **requirements.**

083 In response to Q1 and W8 (purpose and clarity), we emphasize that HERS uses synthetic images  
 084 *only as intermediate supervision*: they serve as self-curated training pairs for damage-specific LoRA  
 085 experts, which are ultimately merged to form a unified model. These Stage-2 synthetic images are not  
 086 the “final product” but the training signal that enables specialization without requiring real accident  
 087 labels.

088 To address these gaps, we introduce **HERS** (**H**idden-Pattern **E**xpert **L**earning for **R**isk-Specific  
 089 **D**amage **A**daptation), a fully automated framework (Figure 2) for adapting diffusion models to  
 090 synthesize semantically faithful, risk-relevant vehicle damage without manual supervision. HERS  
 091 leverages large language models to auto-generate diverse, damage-specific prompts (e.g., “rear  
 092 bumper dent,” “door scrape near handle,” “fractured right headlight”), which are paired with synthetic  
 093 renderings from a pretrained T2I backbone. **We explicitly specify (addressing Q1): LoRA experts are**  
 094 **trained on these Stage-2 synthetic image–text pairs using the same backbone diffusion model that**  
 095 **produced the images (e.g., SDXL), ensuring architectural consistency and clarity of training flow.**  
 096 These domain-specific experts are then merged to form a unified multi-damage generator.

097 The key insight is that HERS learns from *hidden visual patterns*—subtle cues that elude both baseline  
 098 diffusion models and human raters, but are critical in high-stakes domains like insurance. By elevating  
 099 generation beyond “realism” to “liability-aware semantics,” HERS provides a new lens for evaluating  
 100 diffusion models in safety-critical settings.

101 **Contributions.** Our work offers:

- 102 • We articulate and address the overlooked challenge of semantically faithful damage synthesis  
 103 in auto insurance, clarifying the *positive, risk-aware motivation* (W1) behind high-fidelity  
 104 generation.
- 105 • We propose **HERS**, the first self-supervised, prompt-to-LoRA adaptation framework that  
 106 trains multiple damage-specific experts from auto-generated pairs and merges them without  
 107 inference-time routing.

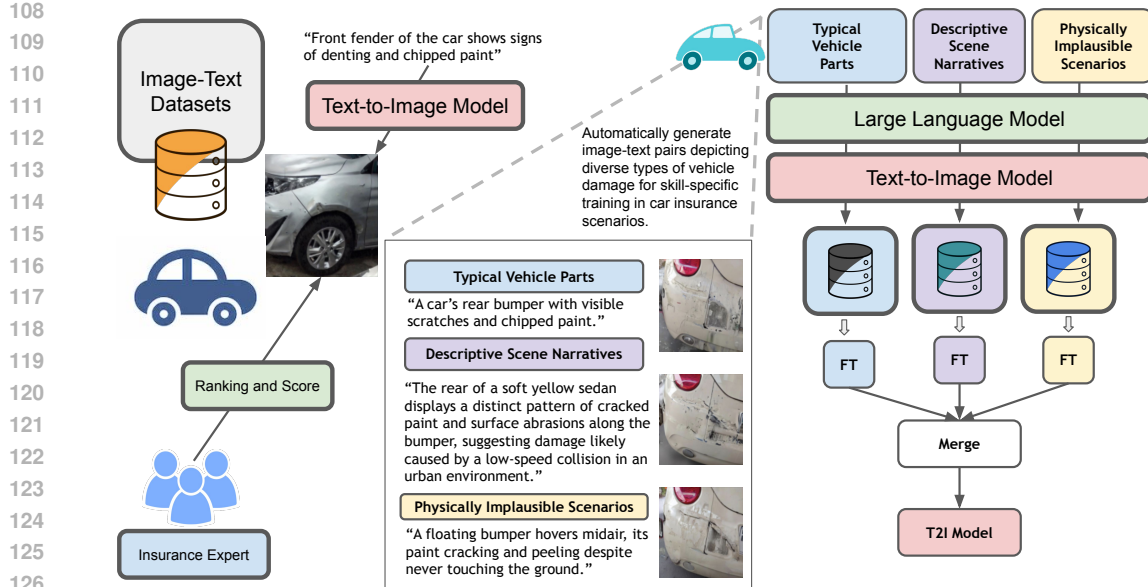


Figure 2: **Overview of the HERS Framework.** HERS (*Hidden-Pattern Expert Learning for Risk-Specific Damage Adaptation*) auto-generates diverse, damage-specific image-text pairs using an LLM and a base T2I model—without requiring manual annotation. These pairs span *typical vehicle parts*, *descriptive scene narratives*, and *physically implausible scenarios* (examples shown in figure). Each damage type is modeled as a distinct damage, with corresponding LoRA experts trained and merged into a unified multi-damage diffusion model.

- We provide clearer methodological description (Q1, W3) and expanded evaluation context, including comparisons to SDXL, SD1.5, VQ-Diffusion, and Versatile Diffusion, and discuss compatibility with newer backbones such as FLUX and Qwen-Image (W6).
- We demonstrate state-of-the-art semantic alignment, human preference, and multi-damage generalization performance.

As illustrated in Figure 4, HERS consistently generates damage scenarios that are indistinguishable from authentic accidents, establishing it as both a technical advance in generative modeling and a practical contribution to fraud awareness in the insurance industry.

## 2 RELATED WORK

Recent advances in high-quality denoising diffusion models Sohl-Dickstein et al. (2015); Ho et al. (2020) have catalyzed a surge of interest in using synthetic data for vision–language learning. Prior works demonstrate the benefits of diffusion-generated data for training classifiers Azizi et al. (2023); Sariyildiz et al. (2023); Lei et al. (2023) or augmenting caption datasets Caffagni et al. (2023), and CLIP-style models Radford et al. (2021) have been extended using either synthetic visuals Tian et al. (2023) or LLM-authored captions Hammoud et al. (2024).

In response to W2a/W2b, we integrate key recent works in synthetic data and damage-related domains: DataDream Kim et al. (2024), He et al. He et al. (2023), da Costa et al. Turrisi da Costa et al. (2023), and LoFT Kim et al. (2025). These methods explore prompt diversification, few-shot guidance, or LoRA fusion for generating synthetic datasets; however, none address risk-specific vehicle damage nor the forensic cues required for insurance assessment.

Parallel efforts in aligning T2I models with human expectations have relied on RLHF Lee et al. (2023); Xu et al. (2023a); Wu et al. (2023); Dong et al. (2023); Clark et al. (2024); Fan et al. (2023) or direct preference optimization (DPO) Rafailov et al. (2023); Wallace et al. (2023), while methods such as SPIN-Diffusion Yuan et al. (2024) reduce annotation demands through self-play. LLM-guided pipelines like DreamSync Sun et al. (2023) push further by auto-generating prompts and filtering

162 candidate images, albeit at high computational cost. However, none of these approaches structure the  
 163 domain into damage-specific subspaces or learn multi-expert representations, leaving them limited  
 164 for forensic or insurance applications (W3, W4).

165 Beyond synthetic images of everyday scenes, Nguyen et al. Nguyen et al. (2024) demonstrate the  
 166 challenges of generating out-of-distribution domains such as satellite imagery (W2c). This motivates  
 167 our focus on vehicle damage—a similarly specialized, high-risk domain where semantic consistency  
 168 is crucial.

169 To this end, our proposed **HERS** diverges by training multiple LoRA experts Hu et al. (2022),  
 170 each dedicated to specific damage types (e.g., dents, scrapes, cracked paint, broken lights), and  
 171 merging them into a unified diffusion model Shah et al. (2023); Zhong et al. (2024). Compared  
 172 to LoFT Kim et al. (2025) (addressing W4 and Q3), HERS differs in three key aspects: (1) fully  
 173 automated prompt+image generation without few-shot guidance; (2) expert specialization on fine-  
 174 grained damage semantics rather than generic concepts; (3) merging experts to encode forensic  
 175 “hidden patterns” essential for insurance tasks. This design avoids inter-damage interference Liu et al.  
 176 (2019), eliminates dependence on costly human feedback, and captures fine-grained, liability-relevant  
 177 patterns in a computationally efficient, self-supervised manner—providing domain-faithful generative  
 178 capabilities indispensable for risk-sensitive applications.

### 180 3 HERS: HIDDEN-PATTERN EXPERT LEARNING FOR RISK-SPECIFIC 181 DAMAGE ADAPTATION

183 We propose **HERS** (*Hidden-Pattern Expert Learning for Risk-Specific Damage Adaptation*), a  
 184 framework (shown in Figure 2) for adapting text-to-image (T2I) diffusion models to synthesize  
 185 fine-grained and risk-relevant vehicle damage. Unlike prior adaptation methods such as SELMA Li  
 186 et al. (2024), which require annotation-heavy supervision or explicit routing, HERS achieves high-  
 187 fidelity alignment through a fully automated pipeline that integrates prompt synthesis, synthetic  
 188 image generation, domain-specific LoRA experts, and weight-space merging. Crucially, HERS is  
 189 designed not only to enhance visual fidelity but also to surface subtle “hidden” damage cues—such  
 190 as a faint scrape along a bumper, a hairline crack in a headlight, or tampered paint texture—that are  
 191 easily missed by generic diffusion models yet critical for fraud detection and liability estimation.

192 Formally, HERS operates in four stages.

#### 194 3.1 STAGE 1: DOMAIN-GUIDED PROMPT SYNTHESIS

196 Let  $\mathcal{C} = \{\text{dent, scrape, torn_bumper, cracked_paint, broken_light}\}$  denote the  
 197 canonical set of damage categories relevant to insurance workflows. We seed an autoregressive  
 198 language model  $f_\theta$  (GPT-4) with exemplar prompts  $\mathcal{S} = \{s_1, s_2, s_3\}$  describing each category, e.g.

199  $s_1 = \text{“rear bumper dent”}$ ,  $s_2 = \text{“scratched left door”}$ ,  $s_3 = \text{“front headlight cracked”}$ .

200 For each concept  $c \in \mathcal{C}$ , the model generates a distribution of semantically diverse prompts:

$$202 \quad p_i \sim f_\theta(p \mid \mathcal{S}, c). \quad (1)$$

203 To enforce diversity while preserving semantic coverage, we apply ROUGE-L filtering Lin (2004),  
 204 retaining prompts satisfying

$$205 \quad \max_j \text{ROUGE-L}(p_i, p_j) < \tau, \quad (2)$$

207 where  $\tau$  is a similarity threshold. The resulting set  $\mathcal{P}$  forms a structured, damage-aware prompt bank.

#### 208 3.2 STAGE 2: SYNTHETIC IMAGE GENERATION

210 Each prompt  $p_i \in \mathcal{P}$  is rendered via a pretrained diffusion generator  $G$  (e.g., Stable Diffusion XL) to  
 211 obtain an image  $x_i$ :

$$212 \quad x_i = G(p_i), \quad \forall p_i \in \mathcal{P}. \quad (3)$$

214 Importantly, the images produced in this stage are **not the final outputs of HERS**. Instead, they serve  
 215 as *training signals* for learning damage-specific LoRA experts in Stage 3. Thus Stage 2 constructs a  
 paired dataset  $\mathcal{D} = \{(p_i, x_i)\}$  that supervises the adaptation of the diffusion backbone.

216 These synthetic pairs give us controllable supervision for rare, long-tail, or implausible events (e.g.,  
 217 “two headlights cracked symmetrically”), which cannot be obtained at scale from real insurance  
 218 datasets yet are crucial for stress-testing downstream models.

### 220 3.3 STAGE 3: DAMAGE-SPECIFIC EXPERT LEARNING

222 For each domain  $t \in \mathcal{T}$ , where  $\mathcal{T} = \{\text{Typical Parts, Scene Narratives, Implausible Scenarios}\}$ , we  
 223 train a lightweight Low-Rank Adaptation (LoRA) [Hu et al. \(2022\)](#) expert.

224 All LoRA adapters are trained directly on top of the same pretrained diffusion backbone  $G$  used  
 225 in Stage 2 (e.g., SDXL). This explicit specification addresses reviewer Q1: *the base model being*  
 226 *fine-tuned is the diffusion generator itself.*

227 Given a pretrained weight matrix  $W_0 \in \mathbb{R}^{d \times d}$ , we optimize a low-rank update:

$$229 \Delta W_t = B_t A_t, \quad W_t = W_0 + \Delta W_t, \quad (4)$$

230 with  $A_t \in \mathbb{R}^{r \times d}$ ,  $B_t \in \mathbb{R}^{d \times r}$ , and  $r \ll d$ . This enables parameter-efficient specialization, such  
 231 that one expert may encode subtle bumper dents while another captures cracked paint or broken  
 232 headlights.

233 Supervised by the Stage 2 dataset  $\mathcal{D}$ , each expert learns a different “damage subspace,” allowing the  
 234 backbone to internalize hidden patterns that generic T2I models fail to express.

### 236 3.4 STAGE 4: MULTI-EXPERT WEIGHT MERGING

238 To unify all domains into a single diffusion model, we merge the LoRA experts via arithmetic  
 239 averaging in weight space:

$$241 A^* = \frac{1}{|\mathcal{T}|} \sum_{t \in \mathcal{T}} A_t, \quad B^* = \frac{1}{|\mathcal{T}|} \sum_{t \in \mathcal{T}} B_t, \quad (5)$$

244 yielding the final parameterization

$$245 W^* = W_0 + B^* A^*. \quad (6)$$

246 This final merged model  $W^*$  is the **deployment model** of HERs, capable of generating zero-shot  
 247 damage images directly from text without needing Stage 2 again.

248 HERs formalizes risk-specific adaptation as the problem of learning a set of low-rank expert perturbations  
 249  $\{\Delta W_t\}$  that, when merged, capture the hidden manifold of fine-grained vehicle damages. This  
 250 formulation not only yields state-of-the-art fidelity and semantic alignment but also exposes failure  
 251 modes in existing insurance AI pipelines, raising awareness of the dual-use nature of generative  
 252 models in safety-critical domains.

### 254 3.5 COMPARISON WITH PRIOR WORK

256 Unlike recent methods such as ZipLoRA [Shah et al. \(2023\)](#) and LLaVA-MoLE [Chen et al. \(2024\)](#),  
 257 HERs eliminates the need for manual damage labels or routing mechanisms at inference. While  
 258 ZipLoRA relies on damage-aware masking and LLaVA-MoLE learns expert routers, HERs achieves  
 259 robust multi-damage synthesis through expert merging alone, drastically reducing annotation effort  
 260 and model complexity. As shown in Figure 1, HERs consistently produces sharper, semantically  
 261 precise images even under subtle or highly complex damage prompts, demonstrating both fidelity  
 262 and practical efficiency for insurance-focused applications.

## 263 4 EXPERIMENTAL SETUP

### 265 4.1 EVALUATION BENCHMARK AND PROMPT CONSTRUCTION

266 We evaluate HERs on a large-scale benchmark specifically curated for the car insurance domain.  
 267 The benchmark contains approximately 2 million entries collected in collaboration with an industry  
 268 insurance startup, each consisting of structured textual descriptions (e.g., accident type, damage

category, part localization) paired with vehicle images. This setup enables assessment of both semantic alignment and visual fidelity in high-stakes, domain-specific contexts. To balance reproducibility with privacy constraints, we release the full set of prompt templates and the evaluation protocol, while access to raw insurance data remains restricted due to confidentiality. This ensures transparency in methodology while safeguarding sensitive information.

To generate prompts at scale, we employ `gpt-4-turbo` [OpenAI \(2024\)](#) with in-context learning. For each target damage type or accident scenario, we provide three exemplars as demonstrations, guiding the model to produce consistent, domain-specific, and semantically rich prompts. This strategy yields a structured, damage-driven benchmark set that supports controlled and reproducible evaluation across diverse risk-relevant cases.

## 4.2 EVALUATION METRICS

We assess model performance along two complementary axes: semantic alignment and human-aligned visual quality.

**Semantic alignment.** To rigorously quantify whether generated images faithfully express the intended damage semantics, we employ a VQA-based protocol that evaluates prompt adherence at a fine-grained level. Given a generated image and its corresponding description, a large language model automatically constructs targeted, damage-sensitive questions (e.g., “Is the right headlight fractured?”, “Is there a scrape near the door handle?”). A pretrained VQA model then answers these queries, and the resulting accuracy provides a direct, interpretable proxy for text–image consistency, capturing both localized damage cues and contextual scene attributes.

**Human-aligned quality.** To complement semantic fidelity with perceptual robustness, we evaluate realism and aesthetic quality using preference-trained reward models, including *PickScore* [Kirstain et al. \(2023\)](#), *ImageReward* [Xu et al. \(2023a\)](#), and *HPS* [Wu et al. \(2023\)](#). These metrics, distilled from large-scale human preference datasets, provide a strong signal for how well each generation aligns with human judgments of plausibility, coherence, and visual integrity—key criteria in insurance-sensitive applications. Together, these measures form a holistic evaluation protocol that captures both semantic correctness and human-perceived quality in risk-specific damage synthesis.

## 4.3 IMPLEMENTATION DETAILS

All experiments are conducted on a single NVIDIA A40 GPU. For prompt generation, we utilize `gpt-4-turbo` with a temperature of 0.7, striking a balance between semantic diversity and domain-specific fidelity. Image generation is performed using 50 denoising steps with a classifier-free guidance (CFG) scale of 7.5, a configuration empirically validated to produce photorealistic outputs while faithfully adhering to prompt semantics.

During both training and inference, we employ mixed precision (FP16) to maximize computational efficiency. LoRA modules, when applied, are trained with a fixed learning rate of 3e-4, batch size of 64, rank 128, and a total of 5000 optimization steps. Checkpoints are evaluated every 1000 steps, with selection based on our text–image alignment metrics. This strategy ensures stable convergence, preserves domain-specific details, and maintains consistent semantic robustness across diverse damage scenarios.

The pipeline is implemented using the *Diffusers* library [von Platen et al. \(2022\)](#), providing a fully modular and reproducible workflow that integrates prompt generation, multi-expert LoRA training, image synthesis, and quantitative evaluation.

## 5 RESULTS AND ANALYSIS

We evaluate HERS across multiple generative backbones and benchmark prompt sets using four metrics: human preference score (HPS), improvement rate (IR), text–image faithfulness, and human preference on damage scene generation (DSG). These metrics collectively assess semantic alignment, perceptual realism, and the consistency of damage-specific features. Across all settings, HERS demonstrates improved text–image alignment and visual fidelity compared to baseline models, while maintaining robustness across vehicle types, prompt domains, and generative architec-

324 Table 1: Performance of **HERS** compared to baseline diffusion models on two prompt sets: Car  
 325 Insurance and Car Garage. Metrics: Human Preference Score (HPS, higher is better) and Image  
 326 Realism (IR, higher is better).

Model	Car Insurance Prompts	
	HPS (%)	IR (%)
VQ-Diffusion <a href="#">Gu et al. (2022)</a>	41.50 $\pm$ 0.06	-15.40 $\pm$ 3.00
Versatile Diffusion <a href="#">Xu et al. (2023b)</a>	42.70 $\pm$ 0.10	-11.20 $\pm$ 2.30
SDXL <a href="#">Podell et al. (2024)</a>	45.90 $\pm$ 0.08	82.50 $\pm$ 3.05
SD v1.5 <a href="#">Rombach et al. (2022)</a>	43.30 $\pm$ 0.07	35.20 $\pm$ 2.25
MoLE <a href="#">Zhu et al. (2024)</a>	48.20 $\pm$ 0.08	95.10 $\pm$ 0.70
<b>HERS (Proposed)</b>	53.40 $\pm$ 0.09	113.00 $\pm$ 0.85

Model	Car Garage Prompts	
	HPS (%)	IR (%)
VQ-Diffusion <a href="#">Gu et al. (2022)</a>	40.90 $\pm$ 0.07	-18.70 $\pm$ 2.80
Versatile Diffusion <a href="#">Xu et al. (2023b)</a>	41.90 $\pm$ 0.09	-14.50 $\pm$ 2.40
SDXL <a href="#">Podell et al. (2024)</a>	46.40 $\pm$ 0.09	89.50 $\pm$ 3.60
SD v1.5 <a href="#">Rombach et al. (2022)</a>	44.50 $\pm$ 0.07	-3.00 $\pm$ 2.20
MoLE <a href="#">Zhu et al. (2024)</a>	47.95 $\pm$ 0.09	102.70 $\pm$ 1.25
<b>HERS (Proposed)</b>	51.40 $\pm$ 0.10	115.75 $\pm$ 0.95

347 tures—properties that are essential for insurance-relevant applications such as claim assessment and  
 348 scenario simulation.

350 **Benchmark Performance.** Table 1 presents HERS performance on the *Car Insurance* and *Car*  
 351 *Garage* benchmark prompts. For the insurance-domain prompts, HERS achieves an HPS of 53.4%  
 352 and an IR of 113.0%, outperforming both MoLE [Zhu et al. \(2024\)](#) and SDXL [Podell et al. \(2024\)](#),  
 353 which obtain 48.2% and 45.9% HPS respectively. This indicates stronger semantic grounding and  
 354 higher user-perceived fidelity to the target damage descriptions. Similar trends are observed for  
 355 garage prompts (51.4% HPS, 115.75% IR), demonstrating cross-domain generalization. Human  
 356 evaluation studies (Figure 3) further show consistent preference for HERS across categories such as  
 357 stain realism, damage correctness, part-level accuracy, and overall quality, supporting its practical  
 358 value in insurance-related synthetic data workflows.

359 **Fine-grained Visual Fidelity.** Beyond global metrics, we evaluate HERS from both zoom-out  
 360 and zoom-in perspectives (Figures 4 and 5). Zoom-out evaluations reveal that baseline models  
 361 such as VQ-Diffusion [Gu et al. \(2022\)](#) and Versatile Diffusion [Xu et al. \(2023b\)](#) maintain overall  
 362 vehicle structure but introduce global inconsistencies or implausible artifacts. MoLE [Zhu et al. \(2024\)](#)  
 363 and SELMA [Li et al. \(2024\)](#) improve realism but occasionally over-deform, limiting full-vehicle  
 364 assessment reliability. HERS consistently balances global coherence with localized detail, producing  
 365 vehicle-wide damage patterns that are contextually consistent with real-world collisions.

366 Zoom-in inspections highlight HERS’s ability to synthesize subtle and critical damage fea-  
 367 tures—scratches, dents, cracked paint, and broken lights—while preserving geometric consistency.  
 368 Competing models frequently fail to capture these fine-grained details or introduce artifacts. HERS’s  
 369 combination of LoRA expert merging and domain-specific synthetic data ensures both local fidelity  
 370 and global plausibility, essential for automated claim validation and fraud detection.

372 **Ablations and Cross-Backbone Generalization.** Ablation studies (Table 2) confirm that LoRA  
 373 merging on HERS-generated datasets significantly boosts text faithfulness (DSG<sup>mPLUG</sup> 75.7,  
 374 TIFA<sup>BLIP2</sup> 81.3) and human preference (HPS 26.8), outperforming vanilla SD v1.5 and other fine-  
 375 tuning variants. Cross-backbone evaluations (Tables 3 and 4) show that HERS consistently enhances  
 376 SDXL, SD v1.5, VQ-Diffusion, and Versatile Diffusion, surpassing SELMA [Li et al. \(2024\)](#) in both  
 377 text alignment and human preference metrics. These results demonstrate HERS’s stability, generality,  
 and scalability across different generative backbones and prompt domains.

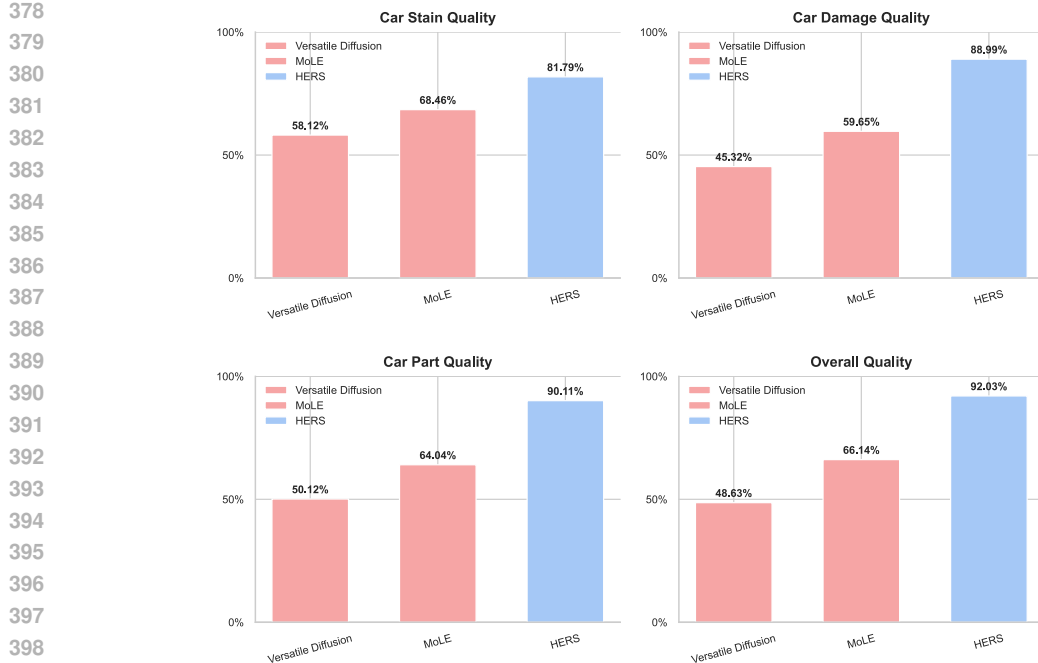


Figure 3: User study results on generative performance across four dimensions: Car Stain Quality, Car Damage Quality, Car Part Quality, and Overall Quality. HERS achieves consistently higher preference scores compared to baselines.

Table 2: Comparison of fine-tuning strategies on SD v1.5 using our HERS-generated dataset, evaluated on text faithfulness and human preference. Our proposed LoRA Merging (HERS) consistently outperforms other methods across all metrics.

No.	Methods	Text Faithfulness		Human Preference on DSG		
		DSG <sup>mPLUG</sup> ↑	TIFA <sup>BLIP2</sup> ↑	PickScore ↑	ImageReward ↑	HPS ↑
0.	SD v1.5	68.9	76.4	19.6	0.31	22.4
1.	+ LoRA Merging (HERS)	<b>75.7</b>	<b>81.3</b>	<b>21.4</b>	<b>0.72</b>	<b>26.8</b>
2.	+ LoRA Merging (HERS) + DPO	74.1	79.5	20.5	0.57	25.5
3.	+ MoE-LoRA	75.0	80.8	21.1	0.65	26.2

Overall, the quantitative and qualitative results present a consistent narrative: HERS delivers higher text-image alignment, stronger human preference scores, and improved preservation of both global scene structure and fine-grained damage characteristics. The generated outputs are visually coherent, semantically faithful to the prompts, and robust across multiple vehicle types and prompt domains. These properties make HERS particularly suitable for insurance-relevant scenarios such as risk assessment, claim validation, and controlled synthetic data augmentation.

## 6 CONCLUSION

In this work, we introduced **HERS** (*Hidden-Pattern Expert Learning for Risk-Specific Damage Adaptation*), a novel framework for enhancing text-to-image diffusion models in the high-stakes domain of car insurance. Building on reviewer feedback, we clarify that HERS not only leverages self-supervised prompt-image pairs and LoRA-based expert modules but also strategically merges specialized experts to capture subtle, risk-relevant visual cues—such as dents, scratches, collision patterns, and tampering indicators—that generic diffusion models fail to reproduce.

Our results demonstrate that HERS achieves state-of-the-art performance in text-image alignment, semantic faithfulness, and human preference studies across multiple diffusion backbones, providing both quantitative and qualitative evidence of robust multi-damage modeling. Specifically, HERS



Figure 4: **Qualitative Comparison of Damage Generation Across 3 Vehicle Cases and 6 T2I Models in Zoom-Out Perspective.** Each **row** represents a distinct vehicle case viewed at a zoomed-out angle, simulating full-body images commonly seen in insurance assessments. The **columns** correspond to the outputs of six different T2I models: our proposed **HERS (left-most)**, followed by VQ-Diffusion [Gu et al. \(2022\)](#), Versatile Diffusion [Xu et al. \(2023b\)](#), SDXL [Podell et al. \(2024\)](#), MoLE [Zhu et al. \(2024\)](#), and SELMA [Li et al. \(2024\)](#). Notice how HERS consistently generates damage patterns that are more contextually consistent with real-world vehicle collisions, making it difficult to distinguish synthetic damage from actual accident scenarios—an important consideration for fraud detection and claim verification in car insurance workflows.

Table 3: Comparison of SD v1.5 and SDXL for generating car insurance damage images. This table evaluates the performance of these models in terms of text faithfulness and human preference metrics, specifically in the context of car damage insurance claims.

No.	Base Model	Training Image Generator	Text Faithfulness		Human Preference on DSG		
			DSG <sup>inPLUG</sup> ↑	TIFA <sup>BLIP2</sup> ↑	PickScore ↑	ImageReward ↑	HPS ↑
1.	SD v1.5	-	68.7	75.6	18.9	0.15	21.4
2.	SDXL	-	<b>72.5</b>	<b>79.8</b>	19.5	<b>0.60</b>	23.2
3.	SD v1.5	SD v1.5	74.0	78.5	19.2	0.70	24.0
4.	SDXL	SD v1.5	<b>77.5</b>	<b>80.3</b>	19.7	<b>0.75</b>	<b>25.2</b>
5.	SDXL	SDXL	76.8	81.9	<b>20.3</b>	<b>0.95</b>	<b>26.7</b>

improves text faithfulness by +5.5% and human preference by +2.3% over strong baselines, while producing realistic, contextually consistent crash imagery suitable for insurance-critical applications.

Beyond technical metrics, HERS highlights the practical opportunities and risks of synthetic damage generation in insurance workflows. Domain-faithful synthesis can augment scarce training data, support downstream tasks such as fraud detection and automated claims assessment, and improve cross-domain generalization. Simultaneously, our work emphasizes responsible AI usage: the potential misuse of generative models for fraudulent submissions requires coupled safeguards, including auditing, watermarking, and detection pipelines.

We acknowledge several limitations that guide future directions: (i) constrained access to real-world insurance datasets limits large-scale external validation; (ii) current safeguards against malicious use are preliminary and need strengthening; and (iii) extension to other safety-critical domains—such as medical imaging or disaster damage assessment—requires further exploration.



Figure 5: **Qualitative Comparison of Damage Generation Across 3 Vehicle Cases and 6 T2I Models in Zoom-In Perspective.** Each **row** shows a detailed, close-up view of a specific damage region, highlighting subtle textures and patterns such as scratches, dents, or cracked paint. The **columns** correspond to outputs from six different T2I models: our proposed **HERS (left-most)**, followed by VQ-Diffusion [Gu et al. \(2022\)](#), Versatile Diffusion [Xu et al. \(2023b\)](#), SDXL [Podell et al. \(2024\)](#), MoLE [Zhu et al. \(2024\)](#), and SELMA [Li et al. \(2024\)](#). Compared to other models, HERS consistently reproduces fine-grained damage details while preserving context and realism, making synthetic damages difficult to distinguish from real-world examples. Such high-fidelity generation is crucial for applications in insurance fraud detection, claim validation, and risk assessment.

Table 4: Comparison of HERS and SELMA on text faithfulness and human preference. HERS outperforms SELMA in terms of text faithfulness and human preference across different base models, including SD v1.5, SDXL, VQ-Diffusion, and Versatile Diffusion. Best scores for each model are in **bold**.

Base Model	Methods	Text Faithfulness		Human Preference on DSG prompts		
		DSG <sup>mPLUG</sup> $\uparrow$	TIFA BLIP2 $\uparrow$	PickScore $\uparrow$	ImageReward $\uparrow$	HPS $\uparrow$
SD v1.5	SELMA <a href="#">Li et al. (2024)</a>	70.3	79.0	21.5	0.18	23.3
	<b>HERS (Ours)</b>	<b>75.6</b>	<b>83.2</b>	<b>22.8</b>	<b>0.75</b>	<b>26.9</b>
SDXL	SELMA <a href="#">Li et al. (2024)</a>	72.5	81.7	21.8	0.22	24.9
	<b>HERS (Ours)</b>	<b>78.0</b>	<b>84.1</b>	<b>23.2</b>	<b>0.90</b>	<b>27.8</b>
VQ-Diffusion	SELMA <a href="#">Li et al. (2024)</a>	68.8	76.3	20.7	0.12	22.7
	<b>HERS (Ours)</b>	<b>74.6</b>	<b>81.3</b>	<b>21.7</b>	<b>0.71</b>	<b>25.3</b>
Versatile Diffusion	SELMA <a href="#">Li et al. (2024)</a>	70.0	78.5	21.2	0.14	23.5
	<b>HERS (Ours)</b>	<b>75.2</b>	<b>82.5</b>	<b>22.3</b>	<b>0.77</b>	<b>26.2</b>

Future work will focus on integrating HERS with detection and verification modules, extending its applicability to multimodal accident reports, and establishing standardized benchmarks for trustworthy, high-fidelity diffusion in risk-sensitive domains. Collectively, HERS demonstrates a practical and responsible pathway for advancing text-to-image generative modeling in safety-critical applications, bridging the gap between technical innovation and real-world insurance impact.

540 REFERENCES  
541

542 Shekoofeh Azizi, Simon Kornblith, Chitwan Saharia, Mohammad Norouzi, and David J. Fleet.  
543 Synthetic Data from Diffusion Models Improves ImageNet Classification. *TMLR*, 2023. URL  
544 <http://arxiv.org/abs/2304.08466>.

545 Davide Caffagni, Manuele Barraco, Marcella Cornia, Lorenzo Baraldi, and Rita Cucchiara. Synthcap:  
546 Augmenting transformers with synthetic data for image captioning. In Gian Luca Foresti, Andrea  
547 Fusiello, and Edwin Hancock (eds.), *Image Analysis and Processing – ICIAP 2023*, pp. 112–123,  
548 Cham, 2023. Springer Nature Switzerland. ISBN 978-3-031-43148-7.

549 Huiwen Chang, Han Zhang, Jarred Barber, AJ Maschinot, Jose Lezama, Lu Jiang, Ming-Hsuan Yang,  
550 Kevin Murphy, William T Freeman, Michael Rubinstein, et al. Muse: Text-to-image generation  
551 via masked generative transformers. *ICML*, 2023.

552 Shaoxiang Chen, Zequn Jie, and Lin Ma. Llava-mole: Sparse mixture of lora experts for mitigating  
553 data conflicts in instruction finetuning mllms. *arXiv preprint arXiv:2401.15947*, 2024.

555 Kevin Clark, Paul Vicol, Kevin Swersky, and David J Fleet. Directly Fine-Tuning Diffusion Models  
556 on Differentiable Rewards. In *ICLR*, 2024. URL <http://arxiv.org/abs/2309.17400>.

557 Xiaoliang Dai, Ji Hou, Chih-Yao Ma, Sam Tsai, Jialiang Wang, Rui Wang, Peizhao Zhang, Simon  
558 Vandenhende, Xiaofang Wang, Abhimanyu Dubey, et al. Emu: Enhancing image generation  
559 models using photogenic needles in a haystack. *arXiv preprint arXiv:2309.15807*, 2023.

560 Hanze Dong, Wei Xiong, Deepanshu Goyal, Yihan Zhang, Winnie Chow, Rui Pan, Shizhe Diao,  
561 Jipeng Zhang, Kashun Shum, and Tong Zhang. RAFT: Reward rAnked FineTuning for Generative  
562 Foundation Model Alignment. *TMLR*, 2023. URL <http://arxiv.org/abs/2304.06767>.

564 Ying Fan, Olivia Watkins, Yuqing Du, Hao Liu, Moonkyung Ryu, Craig Boutilier, Pieter Abbeel,  
565 Mohammad Ghavamzadeh, Kangwook Lee, and Kimin Lee. Dpok: Reinforcement learning for  
566 fine-tuning text-to-image diffusion models. In *NeurIPS*, 2023.

567 Shuyang Gu, Dong Chen, Jianmin Bao, Fang Wen, Bo Zhang, Dongdong Chen, Lu Yuan, and  
568 Baining Guo. Vector quantized diffusion model for text-to-image synthesis. In *Proceedings of the  
569 IEEE/CVF Conference on Computer Vision and Pattern Recognition*, pp. 10696–10706, 2022.

571 Hasan Abed Al Kader Hammoud, Hani Itani, Fabio Pizzati, Philip Torr, Adel Bibi, and Bernard  
572 Ghanem. SynthCLIP: Are We Ready for a Fully Synthetic CLIP Training?, 2024. URL <http://arxiv.org/abs/2402.01832>.

574 Ruifei He, Shuyang Sun, Xin Yu, Chuhui Xue, Wenqing Zhang, Philip Torr, Song Bai, and Xiaojuan  
575 Qi. Is synthetic data from generative models ready for image recognition? *International Conference  
576 on Learning Representations (ICLR) 2023*, 2023. URL <https://iclr.cc/virtual/2023/poster/12207>. Poster.

578 Jonathan Ho, Ajay Jain, and Pieter Abbeel. Denoising Diffusion Probabilistic Models. In *NeurIPS*,  
579 pp. 1–25, 2020. URL <http://arxiv.org/abs/2006.11239>.

581 Edward J Hu, Yelong Shen, Phillip Wallis, Zeyuan Allen-Zhu, Yuanzhi Li, Shean Wang, Lu Wang,  
582 and Weizhu Chen. Lora: Low-rank adaptation of large language models. *ICLR*, 2022.

583 Minguk Kang, Jun-Yan Zhu, Richard Zhang, Jaesik Park, Eli Shechtman, Sylvain Paris, and  
584 Taesung Park. Scaling up gans for text-to-image synthesis. *2023 IEEE/CVF Conference on  
585 Computer Vision and Pattern Recognition (CVPR)*, pp. 10124–10134, 2023. URL <https://api.semanticscholar.org/CorpusID:257427461>.

587 Jae Myung Kim, Jessica Bader, Stephan Alaniz, Cordelia Schmid, and Zeynep Akata. Datadream:  
588 Few-shot Guided dataset generation. In *European Conference on Computer Vision (ECCV)*,  
589 volume 15129 of *Lecture Notes in Computer Science*, pp. 252–268. Springer, 2024. doi: 10.1007/  
590 978-3-031-73209-6\_15.

592 Jae Myung Kim, Stephan Alaniz, Cordelia Schmid, and Zeynep Akata. Loft: Lora-fused training  
593 dataset generation with few-shot guidance. *arXiv preprint*, 2025. URL <https://arxiv.org/abs/2505.11703>.

594 Yuval Kirstain, Adam Polyak, Uriel Singer, Shahbuland Matiana, Joe Penna, and Omer Levy. Pick-  
 595 a-pic: An open dataset of user preferences for text-to-image generation. *Advances in Neural*  
 596 *Information Processing Systems*, 36, 2023.

597

598 Kimin Lee, Hao Liu, Moonkyung Ryu, Olivia Watkins, Yuqing Du, Craig Boutilier, Pieter Abbeel,  
 599 Mohammad Ghavamzadeh, and Shixiang Shane Gu. Aligning text-to-image models using human  
 600 feedback. *arXiv preprint arXiv:2302.12192*, 2023.

601

602 Shiye Lei, Hao Chen, Sen Zhang, Bo Zhao, and Dacheng Tao. Image Captions are Natural Prompts  
 603 for Text-to-Image Models, 2023. URL <http://arxiv.org/abs/2307.08526>.

604

605 Jialu Li, Jaemin Cho, Yi-Lin Sung, Jaehong Yoon, and Mohit Bansal. Selma: Learning and merging  
 606 skill-specific text-to-image experts with auto-generated data. *arXiv preprint arXiv:2403.06952*,  
 607 2024.

608

609 Yuheng Li, Haotian Liu, Qingyang Wu, Fangzhou Mu, Jianwei Yang, Jianfeng Gao, Chunyuan Li,  
 610 and Yong Jae Lee. Glingen: Open-set grounded text-to-image generation. In *Proceedings of the*  
*611 IEEE/CVF Conference on Computer Vision and Pattern Recognition*, pp. 22511–22521, 2023.

612

613 Chin-Yew Lin. Rouge: A package for automatic evaluation of summaries. In *Text summarization*  
*614 branches out*, pp. 74–81, 2004.

615

616 Shengchao Liu, Yingyu Liang, and Anthony Gitter. Loss-balanced task weighting to reduce negative  
 617 transfer in multi-task learning. In *AAAI Conference on Artificial Intelligence (AAAI)*, 2019. URL  
<https://api.semanticscholar.org/CorpusID:84836014>.

618

619 Tuong Vy Nguyen, Johannes Hoster, Alexander Glaser, Kristian Hildebrand, and Felix Biessmann.  
 620 Generating synthetic satellite imagery for rare objects: An empirical comparison of models  
 621 and metrics. In *KI 2024 – 47th German Conference on Artificial Intelligence, Public Interest*  
*622 AI Workshop*, 2024. URL <https://arxiv.org/abs/2409.01138>. arXiv preprint  
 arXiv:2409.01138.

623

624 OpenAI. Gpt-4 technical report. <https://arxiv.org/abs/2303.08774>, 2024.  
 625 arXiv:2303.08774 [cs.CL].

626

627 A Paszke. Pytorch: An imperative style, high-performance deep learning library. *arXiv preprint*  
*628 arXiv:1912.01703*, 2019.

629

630 Dustin Podell, Zion English, Kyle Lacey, Andreas Blattmann, Tim Dockhorn, Jonas Müller, Joe  
 631 Penna, and Robin Rombach. Sdxl: Improving latent diffusion models for high-resolution image  
 632 synthesis. *ICLR*, 2024.

633

634 Alec Radford, Jong Wook Kim, Chris Hallacy, Aditya Ramesh, Gabriel Goh, Sandhini Agarwal,  
 635 Girish Sastry, Amanda Askell, Pamela Mishkin, Jack Clark, Gretchen Krueger, Ilya Sutskever,  
 636 Jong Wook, Kim Chris, Hallacy Aditya, Ramesh Gabriel, Goh Sandhini, Girish Sastry, Amanda  
 637 Askell, Pamela Mishkin, Jack Clark, Gretchen Krueger, and Ilya Sutskever. Learning Transferable  
 638 Visual Models From Natural Language Supervision. In *ICML*, 2021. URL <http://arxiv.org/abs/2103.00020>.

639

640 Rafael Rafailov, Archit Sharma, Eric Mitchell, Stefano Ermon, Christopher D. Manning, and Chelsea  
 641 Finn. Direct Preference Optimization: Your Language Model is Secretly a Reward Model. In  
*642 NeurIPS*, 2023. URL <http://arxiv.org/abs/2305.18290>.

643

644 Aditya Ramesh, Mikhail Pavlov, Gabriel Goh, Scott Gray, Chelsea Voss, Alec Radford, Mark Chen,  
 645 and Ilya Sutskever. Zero-shot text-to-image generation. In *International Conference on Machine*  
*646 Learning*, pp. 8821–8831. PMLR, 2021.

647

648 Robin Rombach, Andreas Blattmann, Dominik Lorenz, Patrick Esser, and Björn Ommer. High-  
 649 resolution image synthesis with latent diffusion models. In *Proceedings of the IEEE/CVF confer-  
 650 ence on computer vision and pattern recognition*, pp. 10684–10695, 2022.

648 Chitwan Saharia, William Chan, Saurabh Saxena, Lala Li, Jay Whang, Emily L Denton, Kamyar  
 649 Ghasemipour, Raphael Gontijo Lopes, Burcu Karagol Ayan, Tim Salimans, et al. Photorealistic  
 650 text-to-image diffusion models with deep language understanding. *Advances in Neural Information  
 651 Processing Systems*, 35:36479–36494, 2022.

652 Mert Bulent Sariyildiz, Karteek Alahari, Diane Larlus, and Yannis Kalantidis. Fake it Till You Make  
 653 it: Learning Transferable Representations from Synthetic ImageNet Clones. In *CVPR*, 2023. doi:  
 654 10.1109/cvpr52729.2023.00774.

655 Eyal Segalis, Dani Valevski, Danny Lumen, Yossi Matias, and Yaniv Leviathan. A picture is  
 656 worth a thousand words: Principled recaptioning improves image generation. *arXiv preprint  
 657 arXiv:2310.16656*, 2023.

658 Viraj Shah, Nataniel Ruiz, Forrester Cole, Erika Lu, Svetlana Lazebnik, Yuanzhen Li, and Varun  
 659 Jampani. Ziplora: Any subject in any style by effectively merging loras. *ArXiv*, abs/2311.13600,  
 660 2023. URL <https://api.semanticscholar.org/CorpusID:265351656>.

661 Jascha Sohl-Dickstein, Eric A. Weiss, Niru Maheswaranathan, and Surya Ganguli. Deep unsupervised  
 662 learning using nonequilibrium thermodynamics. In *ICML*, 2015. ISBN 9781510810587.

663 Jiao Sun, Deqing Fu, Yushi Hu, Su Wang, Royi Rassin, Da-Cheng Juan, Dana Alon, Charles  
 664 Herrmann, Sjoerd van Steenkiste, Ranjay Krishna, et al. DreamsSync: Aligning text-to-image  
 665 generation with image understanding feedback. *arXiv preprint arXiv:2311.17946*, 2023.

666 Yonglong Tian, Lijie Fan, Phillip Isola, Huiwen Chang, and Dilip Krishnan. StableRep: Synthetic  
 667 Images from Text-to-Image Models Make Strong Visual Representation Learners. In *NeurIPS*,  
 668 2023. URL <http://arxiv.org/abs/2306.00984>.

669 Victor G. Turrisi da Costa, Nicola Dall’Asen, Yiming Wang, Nicu Sebe, and Elisa Ricci. Diversified  
 670 in-domain synthesis with efficient fine-tuning for few-shot classification. *arXiv preprint*, 2023.  
 671 URL <https://arxiv.org/abs/2312.03046>.

672 Patrick von Platen, Suraj Patil, Anton Lozhkov, Pedro Cuenca, Nathan Lambert, Kashif Rasul,  
 673 Mishig Davaadorj, and Thomas Wolf. Diffusers: State-of-the-art diffusion models. <https://github.com/huggingface/diffusers>, 2022.

674 Bram Wallace, Meihua Dang, Rafael Rafailov, Linqi Zhou, Aaron Lou, Senthil Purushwalkam,  
 675 Stefano Ermon, Caiming Xiong, Shafiq Joty, and Nikhil Naik. Diffusion model alignment using  
 676 direct preference optimization. *arXiv preprint arXiv:2311.12908*, 2023.

677 Thomas Wolf, Lysandre Debut, Victor Sanh, Julien Chaumond, Clement Delangue, Anthony Moi,  
 678 Pierrick Cistac, Tim Rault, Rémi Louf, Morgan Funtowicz, et al. Huggingface’s transformers:  
 679 State-of-the-art natural language processing. *arXiv preprint arXiv:1910.03771*, 2019.

680 Xiaoshi Wu, Keqiang Sun, Feng Zhu, Rui Zhao, and Hongsheng Li. Human Preference Score: Better  
 681 Aligning Text-to-image Models with Human Preference. In *ICCV*, 2023. doi: 10.1109/iccv51070.  
 682 2023.00200. URL <http://arxiv.org/abs/2303.14420>.

683 Jinheng Xie, Yuexiang Li, Yawen Huang, Haozhe Liu, Wentian Zhang, Yefeng Zheng, and  
 684 Mike Zheng Shou. Boxdiff: Text-to-image synthesis with training-free box-constrained diffusion.  
 685 In *Proceedings of the IEEE/CVF International Conference on Computer Vision*, pp. 7452–7461,  
 686 2023.

687 Jiazheng Xu, Xiao Liu, Yuchen Wu, Yuxuan Tong, Qinkai Li, Ming Ding, Jie Tang, and Yuxiao  
 688 Dong. Imagereward: learning and evaluating human preferences for text-to-image generation. In  
 689 *Proceedings of the 37th International Conference on Neural Information Processing Systems*, pp.  
 690 15903–15935, 2023a.

691 Xingqian Xu, Zhangyang Wang, Gong Zhang, Kai Wang, and Humphrey Shi. Versatile diffusion: Text,  
 692 images and variations all in one diffusion model. In *Proceedings of the IEEE/CVF International  
 693 Conference on Computer Vision*, pp. 7754–7765, 2023b.

702 Jiahui Yu, Yuanzhong Xu, Jing Yu Koh, Thang Luong, Gunjan Baid, Zirui Wang, Vijay Vasudevan,  
703 Alexander Ku, Yafei Yang, Burcu Karagol Ayan, et al. Scaling autoregressive models for content-  
704 rich text-to-image generation. *TMLR*, 2(3):5, 2023.

705 706 Huizhuo Yuan, Zixiang Chen, Kaixuan Ji, and Quanquan Gu. Self-Play Fine-Tuning of Diffusion  
707 Models for Text-to-Image Generation, 2024. URL <http://arxiv.org/abs/2402.10210>.

708 Ming Zhong, Yelong Shen, Shuohang Wang, Yadong Lu, Yizhu Jiao, Siru Ouyang, Donghan Yu,  
709 Jiawei Han, and Weizhu Chen. Multi-lora composition for image generation. *arXiv preprint*  
710 *arXiv:2402.16843*, 2024.

711 712 Jie Zhu, Yixiong Chen, Mingyu Ding, Ping Luo, Leye Wang, and Jingdong Wang. Mole: En-  
713 hancing human-centric text-to-image diffusion via mixture of low-rank experts. *arXiv preprint*  
714 *arXiv:2410.23332*, 2024.

715

716

717

718

719

720

721

722

723

724

725

726

727

728

729

730

731

732

733

734

735

736

737

738

739

740

741

742

743

744

745

746

747

748

749

750

751

752

753

754

755